Inversion Processes in Phosphines and Their Radical Cations: When Is a Pseudo-Jahn−Teller Effect Operative?†

Steven Creve and Minh Tho Nguyen*

Department of Chemistry, University of Leuven, Celestijnenlaan 200F, B-3001 Leuven, Belgium

Received: February 11, 1998; In Final Form: April 15, 1998

The inversion processes in substituted phosphines (R_3P) and their radical cations have been investigated in detail using high-level ab initio molecular orbital and density functional theory calculations. Particular attention has been paid to the understanding of the inversion mechanism. While in PH_3 and methyl derivatives only the classical vertex inversion exists, halogenated phosphines invert through C_{2v} T-shaped transition structures in most neutral species. The pseudo-Jahn−Teller effect in which an $a_1' \otimes e'$ mixing leads a D_{3h} to a C_{2v} T-shaped transition structure is confirmed to be responsible for the edge inversion. This effect is operative upon substitution of, at least, two H atoms of PH_3 by halogen atoms and appears to be largest in F-derivatives. The pseudo-JT effect is reduced in the order F > Cl > Br. In radical cations, the inversion barriers are consistently and substantially reduced, in such a way that in $PCl_3^{\bullet+}$ and $PBr_3^{\bullet+}$ the pseudo-Jahn−Teller effect virtually disappears and the edge inversion no longer exists. The effect of electron correlation on the inversion barriers has also been considered; it is small in hydrides but becomes quite large in halogenated phosphines. The ionization energies of the phosphines under consideration have also been derived.

1. Introduction

Along with internal rotation, molecular inversion occupies an important place in the conformational analysis of chemical species. The barrier heights that conventionally characterize these processes have long been an attractive target for quantum chemical studies from the early days of ab initio molecular orbital calculations.[1,2] Due to several difficulties encountered in experimental determination of inversion barriers, ab initio computations emerged as an economic alternative. The reliability of different molecular orbital methods in determining this property has already been assessed in several earlier reviews.[3−7] As with other properties, the contribution of electron correlation to the barrier height remains, however, an open question.[8,9] On the other hand, the performance of current density functional theory (DFT) in this domain is not fully calibrated yet.

A problem of particular interest concerns the geometry of transition structures (TSs) and thereby the associated mechanism. Ammonia is well established to invert through a D_{3h} TS. The well-expressed "umbrella inversion" became thus a deeply rooted popular wisdom so that the inversion of tricoordinated compounds containing group 15 elements (N, P, As, ...) was believed, up to 1986, to follow a similar path. In fact, earlier studies on NF_3, PF_3, and PCl_3 considered only D_{3h} transition structures, even though the obtained inversion barriers were unrealistically high, and even higher than the corresponding bond energies.[10−12] That was simply due to the lack of characterization by vibrational analyses. Stimulated by the synthesis of molecules containing planar T-shaped pnictogenes, Dixon and co-workers[13] first reported in 1986 the existence of an alternative inversion process in phosphines. They showed that for the series PH_3, PH_2F, PHF_2, and PF_3, while the first two invert through a planar TS **1** having (or close to) D_{3h} symmetry, the latter two molecules invert through a planar T-shaped TS **2** having C_{2v} symmetry.

1 **2**

The first process, **1**, is referred to as "vertex inversion" and the second, **2**, as "edge inversion". This group also extended their study to other centers[13−15] and showed that the T-shaped structures can be stabilized by σ-acceptors in axial positions (**2**, Ax) and π-donors in equatorial positions (**2**, Eq). These findings have further been supported by calculations of other groups.[16−22] More recently a C_{2v} Y-shaped structure, which corresponds to a second-order saddle point connecting two T-shaped structures, has also been located.[16,21]

The preference for C_{2v} T-shaped TSs has been interpreted, within the framework of perturbational MO arguments, involving the HOMO−LUMO gaps.[18,23] Accordingly, the smaller the gap, the larger the inversion barrier. Nevertheless, that argument does not hold for many fluorinated systems. A correlation between the inversion mode and the distance between the lone pair, characterized by a charge center, and the P atom in phosphines has also been found.[24] The smaller this distance, the more favored the edge inversion process **2**. A minimization of repulsion between negative charges accumulated around the three ligands also favors the vertex inversion **1**. Due to the fact that the HOMO of species that undergo edge inversion (such as PF_3) has a_1' symmetry and therefore is not degenerate, the Jahn−Teller effect has for a long time not been evoked. Only recently have Schwerdtfeger and co-workers[17] demonstrated that in trifluorinated species it is an $a_1' \otimes e'$ mixing in the D_{3h} structure **1** that causes a second-order Jahn−Teller distortion leading to the more stable C_{2v} **2** form. Thus, a legitimate question that

† Dedicated to Professor Luc Vanquickenborne on the occasion of his 60th birthday.

* E-mail: minh.nguyen@chem.kuleuven.ac.be.

S1089-5639(98)01083-4 CCC: $15.00
Published on Web 07/18/1998

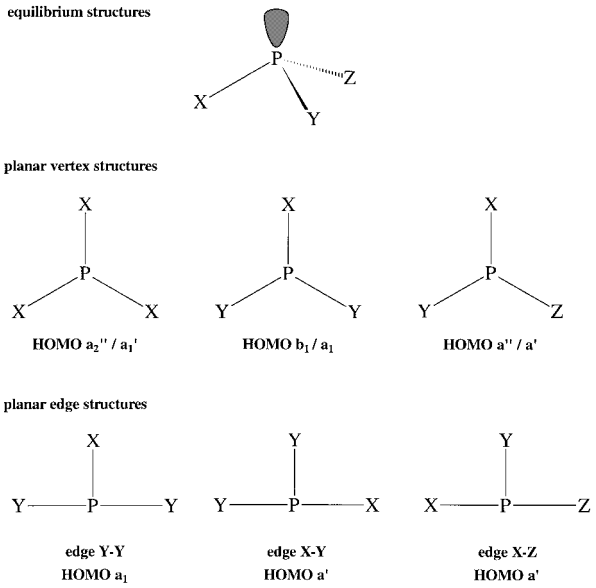

Figure 1. Schematic drawing of the possible structures encountered.

arises in this context is when does this pseudo-Jahn−Teller effect become operative in substituted phosphines.

In the present work, we attempt to tackle the above question in considering a larger series of phosphines that include not only the neutral species but also the corresponding radical cations. Recent calculations[21] have in fact pointed out that although the inversion barrier is strongly reduced upon ionization, the edge inversion remains preferred in $PF_3^{\bullet+}$. In addition, the electron correlation effect on the calculated barriers and ionization energies has also been examined.

2. Computational Details

To explore the various points on the potential energy surfaces, geometries were optimized using the 6-311G(d,p) basis set and both molecular orbital (MP2) and density functionaly theory (B3LYP) methods. The stationary points thus obtained were characterized by harmonic vibrational frequency analyses, at the same levels of theory. A further refinement of the relative energy differences between equilibrium structures, transition structures, and higher order saddle points was reached by single-point calculations of electronic energies using either the B3LYP method or the quadratic configuration interaction [QCISD(T)] method in conjunction with the larger 6-311+G(2df,p) basis set. For the heavier bromine-containing species, optimizations were carried out with the slightly smaller 6-31G(d,p) basis set, QCISD(T) calculations were not feasible, due to a limitation in computational resources. For open-shell systems, the unrestricted formalism has been employed. In general, the UHF references are not particularly contaminated by higher spin states. All calculations were performed with the aid of the Gaussian 94 electronic structure program package.[25]

3. Results and Discussion

3.1. Geometries. Due to the large amount of geometrical data available, we will not mention them in detail here. A full set of optimized parameters for the different structures can however be obtained from the Supporting Information. The different types of structures considered in this study are schematically shown in Figure 1. All ground-state equilibrium structures are calculated to be pyramidal. A few planar minimum structures are also found, which correspond rather to excited states (vide infra). Concerning the planar transition structures, different possibilities arise. As shown in Figure 1, vertex inversion proceeds through a D_{3h} TS or—depending on the substituents—"quasi D_{3h}" C_{2v} and C_s structures. The highest possible symmetry for the T-shaped edge inversion is C_{2v}; other edge structures possess C_s symmetry. We will now briefly discuss some general trends, most of which can be understood in the simple framework of VSEPR theory.

As mentioned above, all ground-state equilibrium structures of phosphines PXYZ are calculated to be pyramidal. As expected, the ∠XPY angle consistently increases by about 10° upon ionization, due to the diminished repulsion with the lone pair on phosphorus.[21]

Two types of vertes TSs exist: while in the first one the lone pair occupies a p_z-type orbital on P (a_2'' in D_{3h}), in the second, an in-plane s-type orbital on P is occupied (a_1' in D_{3h}, Figure 1). In the first case, the P−X bond lengths are shorter as compared with the pyramidal structures; in the latter case, P−X distances increase. This again is in line with the basis of VSEPR.

For the edge structures, the $P-X_{Eq}$ distance is in all cases approximately the same as in the corresponding pyramidal minima. The $P-X_{Ax}$ distance, however, considerably increases (in some cases up to 0.5 Å). This large increase in bond length is due to the lone pair, which is partly delocalized into the $P-X_{Ax}$ bonds.

3.2. Potential Energy Surfaces. In this type of analysis, the identity of each structure is of crucial importance; therefore, Tables 1, 2, 3, 4, and 5 show the imaginary vibrations for all planar structures considered in this study. The displayed wavenumbers are obtained by harmonic frequency analyses, performed at both B3LYP and (U)MP2 levels, in conjunction with the 6-311G(d,p) basis set. For the methyl- and bromine-containing species (Tables 1 and 4), only the 6-31G(d,p) basis was used.

Calculated energy barriers and relative energies are shown in Tables 1−5. For each compound, the displayed energies, given in kJ/mol, are relative with respect to its pyramidal equilibrium structure. The values are corrected for zero-point vibrational energy (ZPE), using a scaling factor of 0.9806[26] for the B3LYP(ZPE) and of 0.94 for MP2(ZPE). Thus, B3LYP energies were calculated using the 6-311G(d,p) and 6-311+G(d,p) and 6-311+G(2df,p) basis sets at the B3LYP optimized geometries. Similarly for MO calculations, both MP2/6-311G(d,p) and QCISD(T)/6-311+G(2df,p) energies were obtained at MP2/6-311G(d,p) geometries.

The following subsections discuss the characteristics of the various planar structures, based upon their imaginary vibrations and relative energies.

3.2.1. PH_3 and $PH_3^{\bullet+}$. Table 2 shows the vibrational frequencies and relative energies of the parent phosphine and its radical cation. In agreement with earlier studies,[13−15] for neutral PH_3, two planar structures were found: a vertex structure in which the lone pair resides in an a_2'' orbital and an edge structure where the lone pair is found in an a_1 orbital. While the vertex structure shows one imaginary vibration corresponding to the umbrella inversion mode, the edge structure has no imaginary frequencies at all. Examination of their orbital occupancies shows the following electronic configurations:

PH_3	C_{3v}	$...(3a_1)^2(4a_1)^2(2e)^4(5a_1)^2$
	vertex D_{3h}	$...(1a_2'')^2(3a'_1)^2(2e')^4(2a_2'')^2$
	edge C_{2v}	$...(3a_1)^{22}(4a_1)^2(2b_2)^2(5a_1)^2(6a_1)^2(2b_1)^0$

Apparently, there is an alteration of orbitals in the C_{2v} T-form.

TABLE 1: Relative Energies (kJ/mol) for the Planar Methyl Structures Considered. In Parentheses Are the Symmetries and Values of the Imaginary Frequencies

		6-31G(d,p)		B3LYP
HOMO		B3LYP	MP2	6-311+G(2df,p)
PH_2CH_3				
C_s	a″	142.4 (a″ 967i)	148.4 (a″ 1015i)	140.4
Cs H−Me	a′	577.9 (a″ 274i)	624.7 (a″ 256i)	557.7
$PH(CH_3)_2$				
C_{2v}	b_1	150.1 (b_1 832i)	159.2 (b_1 870i)	148.4
Cs H−Me	a′	533.5 (a″ 141i)	580.4 (a″ 122i)	511.9
C_{2v} Me−Me	a_1	537.6 (b_1 216i, a_2 193i)	585.1 (b_1 216i, a_2 178i)	518.4
$P(CH_3)_3$				
C_{3v}	a_1	169.9 (a_1 416i, e 29i)	182.9 (a_1 423i)	171.0
C_{3h}	a″	171.6 (a″ 430i, a″ 73i)	184.2 (a″ 437i, a″ 81i)	172.2
$PH_2CH_3^{\bullet+}$				
C_s	a″	11.3 (a″ 564i, a″ 28i)	14.3 (a″ 645i)	12.8
C_s H−Me	a′	314.2 (a″ 1308i, a″ 164i)	304.9 (a″ 171i, a″ 24i)	309.4
$PH(CH_3)_2$				
C_{2v}	b_1	16.2 (b_1 505i)	20.4 (b_1 590i)	18.0
C_s H−Me	a′	324.5 (a″ 92i)	315.3	
$P(CH_3)_3$				
C_{3h}	a″	23.7 (a″ 259i)	30.9 (a″ 302i)	26.0

TABLE 2: Relative Energies (kJ/mol) for the Planar Fluoride Structures Considered. In Parentheses Are the Symmetries and Values of the Imaginary Frequencies

		6-311G(d,p)		6-311+G(2df,p)	
HOMO		B3LYP	MP2	B3LYP	QCISD(T)
PH_3					
D_{3h}	a_2″	137.8 (a_2″ 1085i)	144.6 (a_2″ 1147i)	138.6	141.3
C_{2v}	a_1	618.2 (−)	656.7 (−)	605.2	522.5
PH_2F					
C_{2v}	b_1	211.5 (b_1 1258i)	226.7 (b_1 1346i)	213.0	215.3
C_{2v}	a_1	465.2 (−)	500.3 (−)	459.4	466.6
C_s	a′	343.6 (a″ 1867i)	377.8 (a″ 2020i)	341.0	351.4
PHF_2					
C_{2v}	b_1	364.8 (b_1 1427i)	391.0 (b_1 1490i)	364.8	358.5
C_{2v}	a_1	200.9 (b_1 356i)	226.1 (b_1 389i)	199.2	210.9
C_s	a′	314.6 (a″ 1391i)	344.0 (a″ 1425i)	314.1	323.6
PF_3					
D_{3h}	a_2″	633.6 (a_2″ 1120i)	667.3 (a_s″ 593i)	652.4	446.0
D_{3h}	a_1′	326.3 (a_2″ 578i, e′ 203i)	368.5 (a_2″ 547i, e′ 215i)	328.0	352.8
C_{2v}	a_1	208.7 (b_1 315i)	233.7 (b_1 334i)	208.5	221.1
$PH_3^{\bullet+}$					
D_{3h}	a_2″	8.8 (a_2″ 639i)	11.4 (a_2″ 739i)	8.7	8.6
C_{2v}	a_1	363.8 (−)	399.5 (−)	355.9	368.2
$PH_2F^{\bullet+}$					
C_{2v}	b_1	41.0 (b_1 942i)	47.4 (b_1 1117i)	41.1	41.4
C_{2v}	a_1	268.6 (−)	297.6 (−)	261.1	274.3
C_s	a′	262.3 (−)	288.3 (−)	261.1	271.8
$PHF_2^{\bullet+}$					
C_{2v}	b_1	123.2 (b_1 1366i)	137.1 (b_1 1863i)	122.7	76.0
C_{2v}	a_1	168.4 (b_1 636i)	191.1 (b_1 743i)	172.9	137.1
C_s	a′	178.6 (a″ 1318i)		177.0	
$PF_3^{\bullet+}$					
D_{3h}	a_2″	300.1 (−)	298.0 (−)	310.1	296.1
D_{3h}	a_1′	158.8 (a_2″ 916i, e′ 88i)	210.8 (e′ 68i)	161.3	204.1
C_{2v}	a_1	143.7 (b_1 515i)	173.9 (b_1 549i)	147.2	167.9

A transfer of two electrons from the $2b_1$ to the $6a_1$ orbital occurs. This suggests that the latter is actually not a TS as assumed in ref 13, but rather the equilibrium structure of a lower lying excited state of PH_3. This excited state, if any, is characterized by a transition energy of about 5.4 eV (Table 2).

A similar situation arises for $PH_3^{\bullet+}$. Hence, both PH_3 and $PH_3^{\bullet+}$ undergo inversion via the classical umbrella mechanism. The energy barrier for this inversion is, however, considerably lowered for the cationic species. As a matter of fact, the estimates based on QCISD(T) calculations suggest a value of 141 kJ/mol for PH_3 but only 9 kJ/mol for $PH_3^{\bullet+}$. In a following section, the correlation effect on the barrier will be discussed in some detail. No accurate experimental data have been available yet. For PH_3, values of 115−133 kJ/mol have been suggested more than 40 years ago.[27] Use of an effective inversion potential function[28] to fit the rotation−vibration bands of PH_3 led to an effective inversion barrier of 135 kJ/mol. Earlier CISDQ/TZP calculations resulted in a slightly larger value of 144 kJ/mol.[29]

From a vibrational analysis of the first band of the photoelectron spectrum of PH_3, the inversion barrier of $PH_3^{\bullet+}$ was tentatively proposed as 8 kJ/mol.[30] Larger values were obtained from earlier MO calculations, namely, 15 kJ/mol by CASSCF-CI[31] and 12 kJ/mol by SCF-CISD calculations.[32] As for another comparison, we note that the first adiabatic ionization energy $IE_a(PH_3) = 9.68$ eV, computed using QCISD(T). This value

TABLE 3: Relative Energies (kJ/mol) for the Planar Chloride Structures Considered. In Parentheses Are the Symmetries and Values of the Imaginary Frequencies

		6-311G(d,p)		6-311+G(2df,p)	
HOMO		B3LYP	MP2	B3LYP	QCISD(T)
PH_2Cl					
C_{2v}	b_1	187.4 (b_1 1145i)	194.2 (b_1 1206i)	184.6	185.6
C_s	a′	297.1 (a″ 1512*i*)	355.2 (a″ 2300i)	310.6	324.8
$PHCl_2$					
C_{2v}	b_1	255.9 (b_1 1121i)	261.1 (b_1 1149i)	251.6	248.7
C_{2v}	a_1	175.5 (b_1 270i)	220.5 (b_1 332i)	181.3	203.1
C_s	a′	283.4 (a″ 1363i)	337.6 (a″ 1956i)	293.2	313.8
PCl_3					
D_{3h}	a_2''	347.8 (a_2'' 656i)	350.1 (a_2'' 629i)	342.6	328.4
D_{3h}	a_1'	214.2 (a_2'' 403i, e′ 73i)	270.6 (e′ 61i)	227.8	269.1
C_{2v}	a_1	181.7 (b_1 261i)	226.6 (b_1 230i)	187.1	211.5
$PH_2CL^{\bullet+}$					
C_{2v}	b_1	30.5 (b_1 783i)	31.3 (b_1 882i)	29.4	27.8
C_{2v}	a_1	282.9 (−)	310.4 (−)	272.8	283.3
C_s	a′	241.4 (−)	277.7 (−)	244.3	253.3
$PHCl_2^{\bullet+}$					
C_{2v}	b_1	60.2 (b_1 851i)	60.5 (b_1 975i)	59.6	57.6
C_{2v}	a_1	144.2 (b_1 882i)	186.0 (−)	147.9	169.5
C_s	a′	205.0 (−)	236.1 (−)	208.4	213.2
$PCl_3^{\bullet+}$					
D_{3h}	a_2''	98.0 (a_2'' 649i)	100.3 (a_2'' 784i)	99.0	99.0
D_{3h}	a_1'	117.1 (a_2'' 1321i)	160.4 (−)	122.3	149.2
C_{2v}	a_1	117.2 (b_1 682i)	161.3 (−)	122.2	145.8

TABLE 4: Relative Energies (kJ/mol) for the Planar Bromide Structures Considered. In Parentheses Are the Symmetries and Values of the Imaginary Frequencies

		6-31G(d,p)		6-311+G(2df,p)	
HOMO		B3LYP	MP2	B3LYP	QCISD(T)
PH_2Br					
C_{2v}	b^1	179.4 (b_1 1111i)	186.5 (b_1 1172i)	179.9	179.6
C_s	a′	294.1 (a″ 1681i)	341.5 (a″ 2474i)	286.8	294.4
$PHBr_2$					
C_{2v}	b_1	228.7 (b_1 1052i)	238.0 (b_1 1087i)	230.9	
C_{2v}	a_1	159.9 (b_1 228i)	197.1 (b_1 267i)	164.4	
C_s	a′	272.3 (a″ 1439i)	318.6 (a″ 2211i)	266.9	
PBr_3					
D_{3h}	a_2''	285.7 (a_2'' 581i)	295.4 (a_2'' 553i)	291.4	
D_{3h}	a_1'	181.9 (a_2'' 356i, e′ 25i)	227.8 (e′ 11i)	184.6	
C_{2v}	a_1	161.0 (b_1 227i)	195.7 (b_1 225i)	165.9	
$PH_2Br^{\bullet+}$					
C_{2v}	b_1	28.4 (b_1 735i)	26.7 (b_1 818i)	28.9	
C_s	a′	221.6 (−)	284.6 (−)	222.5	
$PHBr_2^{\bullet+}$					
C_{2v}	b_1	49.9 (b_1 757i)		50.9	
C_{2v}	a_1	115.9 (b_1 698i)		124.8	
$PBr_3^{\bullet+}$					
D_{3h}	a_2''	72.3 (a_2'' 532i)		77.4	
D_{3h}	a_1'	86.4 (a_2'' 1133i)		94.1	

can be compared with the PES values of 9.87 eV[31] and 9.96 eV.[30]

Another point of interest concerns the vibrational wavenumbers associated with the symmetrical bending of $PH_3^{\bullet+}$. The scaled B3LYP and UMP2 values amount to 627 and 689 cm^{-1}, respectively. These are larger than the fitted value[30] of 530 ± 80 cm^{-1} or the CISD value[32] of 522 ± 66 cm^{-1}, but much better than a SCF value of 291 cm^{-1} reported in ref 33. For the purpose of comparison, note that UHF/6-31G(d,p) calculations also provide a large value of 780 cm^{-1} (scaled by 0.9) for this bending mode.

In summary, it can be concluded that both the parent PH_3 and $PH_3^{\bullet+}$ species follow vertex inversion, for which the barrier heights amount to 141 and 9 kJ/mol, respectively, with a probable error of ±5 kJ/mol.

3.2.2. Methyl Substitution. For the methyl-substituted structures, great difficulties were encountered in searching for edge-like transition structures. Probably, this relates to their intrinsic preference for vertex inversion on one hand and to their lower symmetry on the other hand. As such, some of the edge forms resolved under symmetry constraints contain imaginary vibrations corresponding to symmetry lowering. By releasing the symmetry constraints, however, the edge forms could no longer be located. This is the case for the edge Me−Me structure of $PH(CH_3)_2$ and the edge H−Me structure of $PH_2CH_3^{\bullet+}$. In the $PH_2CH_3^{\bullet+}$ case, even the vertex structure has two imaginary wavenumbers at the B3LYP level. One of them, which is very small (28 cm^{-1}) but does not belong to the motion of a methyl group, disappears however at the MP2 level. Analogous behavior is also observed for the C_{3v} vertex form of $P(CH_3)_3$, where B3LYP predicts a degenerate imaginary e-mode, which again disappears at the MP2 level. Hence, this could be due to a B3LYP deficiency. For its part, the C_{3h} vertex form of $P(CH_3)_3$ shows two imaginary modes at both the B3LYP

TABLE 5: Relative Energies (kJ/mol) for the Planar Mixed Structures Considered. In Parentheses Are the Symmetries and Values of the Imaginary Frequencies

		6-311G(d,p)		6-311+G(2df,p)	
HOMO		B3LYP	MP2	B3LYP	QCISD(T)
PF_2Cl					
C_{2v}	b_1	521.6 (b_1 965i)	544.1 (b_1 865i)	520.9	455.4
C_{2v}	a_1	215.3 (b_1 330i)	242.9 (b_1 353i)	211.9	225.5
C_s	a′	189.0 (a″ 280i)	221.8 (a″ 306i)	193.7	210.9
$PFCl_2$					
C_{2v}	b_1	427.6 (b_1 808i)	439.4 (b_1 775i)	420.7	394.0
C_{2v}	a_1	177.5 (b_1 232i)	218.2 (b_1 261i)	183.5	205.1
C_s	a′	195.2 (a″ 306i)	231.8 (a″ 339i)	199.0	217.0
PHFCl					
C_s	a″	305.7 (a″ 1269i)	320.4 (A″ 1318i)	301.4	297.7
C_s H−F	a′	330.2 (a″ 1608i)	363.0 (a″ 1675i)	323.2	334.4
C_s H−Cl	a′	280.6 (a″ 1251i)	327.1 (a″ 1538i)	291.5	309.5
C_s F−Cl	a′	184.0 (a″ 319i)	219.2 (a″ 366i)	189.4	204.4
PFClBr					
C_s	a″	401.7 (a″ 813i)		394.2	
C_s F−Cl	a′	192.2 (a″ 303i)		198.2	
C_s F−Br	a′	186.3 (a″ 304i)		187.5	
C_sCl−Br	a′	168.6 (a″ 219i)		173.2	
$PF_2Cl^{\bullet+}$					
C_{2v}	b_1	189.2 (b_1 1788i)	208.3 (b_1 1409i)	190.8	200.9
C_{2v}	a_1	151.8 (b_1 583i)	180.9 (b_1 241i)	156.0	176.2
C_s	a′	127.6 (a″ 447i)	167.2 (−)	131.0	152.7
$PFCl_2^{\bullet+}$					
C_{2v}	b_1	137.5 (b_1 986i)	146.8 (b_1 1660i)	137.8	140.9
C_{2v}	a_1	117.4 (b_1 440i)	177.7 (−)	120.0	160.2
C_s	a′	131.3 (a″ 547i)	190.4 (−)	136.9	177.5
$PHFCl^{\bullet+}$					
C_s	a″	86.4 (a″ 1071i)	92.2 (a″ 1308i)	85.1	85.2
C_s H−F	a′	194.9 (a″ 2140i)	276.2 (−)	191.9	259.5
C_s H−Cl	a′	183.4 (a″ 3386i)	232.2 (−)	182.6	211.8
C_s F−Cl	a′	156.9 (a″ 703i)	196.0 (−)	159.8	183.7
$PFClBr^{\bullet+}$					
C_s	a″	126.3 (a″ 941i)		126.0	
C_s F−Br	a′	113.6 (a″ 479i)		118.1	
C_s Cl−Br	a′	104.8 (a″ 398i)		107.5	

and MP2 levels. Attempts to relax the C_{3h} structure by following the second mode invariably resulted in a structure converged to either C_{3v} or C_s symmetry. For both $P(CH_3)_3$ and $P(CH_3)_3^{\bullet+}$ structures, we have not been able to locate any edge inversion TS.

From Tables 1 and 2 it is seen that in all cases the inversion barriers of $PH_x(CH_3)_y$, with $x + y = 3$, closely resemble those of PH_3, both in neutral and cationic forms. For $P(CH_3)_3$, the present values are smaller than earlier SCF values of 186−203 kJ/mol.[34] Moreover, upon increasing methyl substitution, only a small increase in the inversion barrier of the vertex forms is noticed, while for the halogen-containing structures, as we shall see in following sections, such an increase is clearly seen. This is also in line with the trend seen in methyl-substituted amines, where the inversion barrier at nitrogen is not affected by the first two methyl groups but slightly increased by the third methyl.[35] The experimental barriers for NH_3 and $N(CH_3)_3$ amount in fact to 24 and 34 kJ/mol, respectively.[36] Hence, one may conclude that methyl substitution has a small influence on the inversional behavior of phosphines, and thus methyl-containing structures most probably undergo inversion through classical vertex transition states.

3.2.3. Fluorine Substitution. The effect of substitution of H atoms by F atoms in PH_3 and $PH_3^{\bullet+}$ is summarized in Table 2. As seen from the imaginary vibrations, PH_2F is confirmed to undergo both vertex and edge H−F inversion.[13−15] The edge H−H structure likely corresponds to a minimum on an excited-state energy surface. The vertex inversion of PH_2F is however favored over the edge H−F by about 136 kJ/mol. A different situation is found for $PH_2F^{\bullet+}$, were only the vertex structure corresponds to a transition state for inversion. Both edge forms are to be considered as excited-state minima.

Further substitution of a H atom yields PHF_2 and $PHF_2^{\bullet+}$. Here, for the neutral PHF_2, inversion via the edge F−F form is the lowest energy path, followed by the edge H−F path and then the vertex inversion. While these three possible inversion pathways also exist for cationic $PHF_2^{\bullet+}$, the most favorable way is still inversion through a vertex form. A few additional points are noteworthy at this stage.

(i) Substitution of two H atoms by F atoms (PHF_2) makes the edge inversion more favorable than vertex inversion.

(ii) PHF_2 and $PHF_2^{\bullet+}$ undergo inversion via different paths: while the neutral prefers edge inversion, the ion proceeds through a vertex transition structure.

(iii) For $PHF_2^{\bullet+}$ an edge H−F form was found using B3LYP but not with MP2 geometry optimizations.

Finally we consider the perfluorinated PF_3 and $PF_3^{\bullet+}$ species. These species were thoroughly studied in recent work.[21] It is found that for trigonal planar PF_3 (D_{3h} symmetry) the lone pair is most likely located in an a_1' orbital. The D_{3h} form with an a_2'' HOMO is ±300 kJ/mol higher in energy. This change in HOMO symmetry will be discussed in a further subsection. While the D_{3h} a_2'' form of PF_3 has only one imaginary vibration corresponding to inversion, the D_{3h} a_1' form has three imaginary wavenumbers. The a_2'' mode corresponds to inversion, while the degenerate e' mode results in symmetry lowering from D_{3h} to C_{2v}. This is related to pseudo-Jahn−Teller effect, which we will come back to in a further section. The T-shaped edge inversion structure then corresponds to the lowest energy inversion path of PF_3. The same behavior is found for $PF_3^{\bullet+}$, although two additional remarks seem necessary here:

(i) For the D_{3h} vertex form, two electronic states could be located, one in which the single electron resides in a a_1' orbital and another in which it resides in an a_2'' p-orbital on P. The former is the direct analogue of the D_{3h} form found for PF_3; the latter has no imaginary vibrations and hence is probably an excited state of $PF_3^{\bullet+}$.

(ii) For the D_{3h} vertex form where the unpaired electron occupies an a_1' orbital, B3LYP yields three imaginary vibrations, while the MP2 method only two (a degenerate e' mode). It turns out that the inversion mode has disappeared at the MP2 level. As stated in our previous study[21] where CISD frequencies were also included, it is not clear whether this is due to a B3LYP problem or an MP2 deficiency.

3.2.4. Chlorine Substitution. The chlorine effect on vibrational wavenumbers and relative energies is shown in Table 3. For the monosubstituted PH_2Cl two possible inversion pathways are found: a low-energy vertex path and a higher energy edge H−Cl path. An edge H−H structure was not found. For its radical counterpart, $PH_2Cl^{\bullet+}$, both edge H−H and edge H−Cl structures are located. Again they probably correspond to minima on excited-state surfaces. Hence the $PH_2Cl^{\bullet+}$ can only undergo inversion through the vertex path.

The doubly substituted $PHCl_2$ is seen to have three possible inversion mechanisms. Similar to PHF_2, an edge Cl−Cl path is the most favorable, followed by a vertex and an edge H−Cl path. While these three structures are also calculated for the cationic $PHCl_2^{\bullet+}$ species, the vertex path is in this case clearly the lowest energy path. Note also that for the cationic species the edge H−Cl structure corresponds to a minimum. The edge Cl−Cl form, however, is a transition structure at the B3LYP level but actually a minimum at the MP2 level.

PCl_3 behaves in the same way as PF_3. Two vertex forms of D_{3h} symmetry are located in which the HOMOs are of $a_2''$and

a_1' symmetry. The energy difference between these two forms, however, is much smaller than in PF_3. The vertex form with a_2'' HOMO has one imaginary vibration corresponding to inversion. As with PF_3, the latter form has three imaginary wavenumbers, namely, an a_2'' mode and a degenerate e' mode. At the MP2 level however, the a_2'' inversion mode disappears and only the e' symmetry lowering vibration is left over. An edge structure is also found which clearly corresponds to the lowest energy inversion path. A different situation arises for the cationic $PCl_3^{\bullet+}$. The B3LYP level predicts three possible inversion structures: a D_{3h} vertex form with an a_2'' HOMO, at about 98 kJ/mol above the pyramidal form, a vertex form with an a_1' HOMO, and an edge form. The latter two are somewhat higher in energy, both at about 117 kJ/mol. At the MP2 level, it turns out that only the D_{3h} vertex form with a_2'' HOMO symmetry corresponds to a true transition structure. The other forms are predicted to be excited-state minima.

At this stage, it can be mentioned that the chlorine-containing phosphines have barriers ranging approximately between those of the unsubstituted structures and the fluorine-containing species. Note that the electronegativity of Cl is 3.0, lying in between H (2.1) and F (4.0).

3.2.5. Bromine Substitution. The results of substituting H by Br, the least electronegative element of the halogen atoms considered in this study, are shown in Table 4.

For PH_2Br, both a vertex and edge H−Br TS can be found. It is clear from Table 4 that the vertex is favored over the edge inversion by more than 100 kJ/mol. The cationic $PH_2Br^{\bullet+}$ species behaves exactly in the same manner, with the energy difference amounting to nearly 200 kJ/mol in favor of the vertex TS.

The doubly substituted $PHBr_2$ species also shows three distinct TSs at both B3LYP and MP2 levels of theory: a vertex form and both edge H−Br and edge Br−Br forms. However, Table 4 clearly points out that only the latter edge Br−Br path is energetically feasible. For the cationic $PHBr_2^{\bullet+}$ we were not able to locate an edge H−Br form, and the vertex form turns out to be the most favorable way for inversion, in contrast to the neutral $PHBr_2$.

The trigonal planar D_{3h} form of PBr_3 possesses an a_1' HOMO, while the form with an a_2'' HOMO is more than 100 kJ/mol higher in energy. The most favorable planar structure, however, is the edge form, which is about 20 kJ/mol lower in energy than the D_{3h} form with an a_1' HOMO. Concerning the number and nature of imaginary frequencies, we refer to PCl_3, which is completely analogous. The methods employed in this study were not able to resolve the existence of an edge structure for $PBr_3^{\bullet+}$. Hence, it should be concluded from Table 4 that inversion in neutral perbromophosphine proceeds via an edge TS, while the cationic form prefers a vertex TS having an a_2'' SOMO. In addition, the energy barriers to inversion for $PBr_3^{\bullet+}$ are low, and the difference between both vertex forms with a_2'' SOMO and a_1' SOMO is only 17 kJ/mol.

3.2.6. Mixed Substitution. A few selected phosphines with substitution by different halogen atoms were also calculated. The results are shown in Table 5. The structures under consideration are PF_2Cl, $PFCl_2$, PHFCl, PFClBr, and their radical cations.

It is seen from Table 5 that for the neutral species all possible planar structures possess only one imaginary vibration, which corresponds in all cases to the inversion mode. Hence, the relative energies shown in Table 5 point out the identity of the lowest energy inversion path. Accordingly, PF_2Cl chooses the edge F−Cl form, whereas $PFCl_2$ inverts through an edge Cl−Cl structure. It seems thus that in both cases the most electronegative element, F, tends to occupy an equatorial position (cf. **2**). For PHFCl, however, it turns out that the structure with **H** in equatorial position (edge F−Cl) is the most favorable pathway for inversion, while PFClBr again chooses the edge Cl−Br form for inversion, putting F in equatorial position. It appears thus that both H and F, which bear a larger charge concentration, prefer a position opposite the P lone pair. When both H and F are present, H seems to prevail.

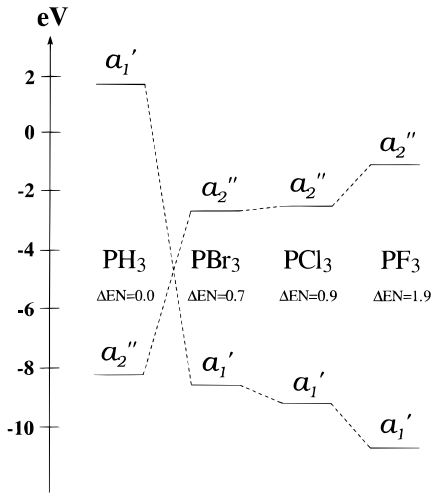

Figure 2. HOMO−LUMO energy difference in planar vertex PH_3, PBr_3, PCl_3, and PF_3. ΔEN is the difference in electronegativity of P and X atoms.

A quite different situation arises for the ionized species. At the B3LYP level of theory, again all planar structures each have one imaginary vibration corresponding to inversion. However, several edge forms considered show no imaginary vibrations at all when calculated at the MP2 level. For $PF_2Cl^{\bullet+}$, a comparison of relative energies points out that inversion proceeds through an edge F−Cl form, thus having an F atom in equatorial position. The $PFCl_2^{\bullet+}$ radical cation turns out to be a problematic case. While B3LYP predicts inversion via an edge Cl−Cl form, both MP2 and QCISD(T) predict inversion via the classical vertex path. For $PHFCl^{\bullet+}$, there is again uniform agreement between the employed methods, revealing that inversion proceeds through the vertex structure. $PFClBr^{\bullet+}$ was only treated at the B3LYP level because of limited computational resources. An edge F−Cl form could not be located, and hence inversion should happen via the edge Cl−Br form, identically to PFClBr.

3.3. The Change in HOMO Symmetry. It is instructive to examine the HOMO of phosphines that are associated with the P lone pair. The change in HOMO symmetry within the series of planar D_{3h} structures PH_3, PBr_3, PCl_3, and PF_3 can be rationalized in terms of electronegativity. A similar analysis was recently done by Schwerdtfeger,[17] for the series NF_3, PF_3, AsF_3, SbF_3, and BiF_3. In that series, only NF_3 has an a_2'' HOMO, while the other compounds have their lone pair in an a_1' HOMO. These authors[17] explained the change in HOMO symmetry in terms of the ionic character of the M−X bond and, hence, the difference in electronegativity (ΔEN(M−X)). The increasing ΔEN on going from NF_3 to PF_3 yields an increased ionic character of the M−X bond. Hence, phosphorus p-orbitals get depopulated in favor of F p-orbitals, which in turn destabilizes the central a_2'' orbital and stabilizes the a_1' orbital. The same reasoning naturally applies to the halogen series PH_3, PBr_3, PCl_3, and PF_3. Figure 2 displays the HOMO−LUMO gaps for the planar D_{3h} structures, together with the

TABLE 6: Summary of the Preferred Inversion Pathways, Correlation Corrections to the Energy Barriers, and Adiabatic Ionization Energies

	neutral			cation			IE_a[d]	
species	inversion[a]	barrier[b]	c.c.[c]	inversion[a]	barrier[b]	c.c.[c]	calc.	pred.
PH_3	v (a_2'')	141.3	−6.6	v (a_2'')	8.6	−8.0	9.68	(9.87)
PH_2CH_3	v (a'')	140.4[e]		v (a'')	12.8[e]		8.92[e]	8.92
$PH(CH_3)_2$	v (b_1)	148.4[e]		v (b_1)	18.0[e]		8.22[e]	8.22
$P(CH_3)_3$	v (a_1)	171.0[e]		v (a'')	26.0[e]		7.72[e]	7.72
PH_2F	v (b_1)	215.3	−22.3	v (b_1)	41.4	−14.5	9.89	10.14
PHF_2	e F−F (a_1)	210.9	−57.0	v (b_1)	76.0	−72.7	10.28	10.53
PF_3	e (a_1)	221.1	−63.8	3 (a_1)	167.9	−60.8	11.29	(11.57)
PH_2Cl	v (b_1)	185.6	−17.2	v (b_1)	27.8	−9.8	9.58	9.83
$PHCl_2$	e Cl−Cl (a_1)	203.1	−49.8	v (b_1)	57.6	−12.0	9.58	9.83
PCl_3	e (a_1)	211.5	−63.8	v (a_2'')	99.0	−14.2	9.72	9.97
PH_2Br	v (b_1)	179.6	−16.1	v (b_1)	28.9[e]		9.50[e]	9.50
$PHBr_2$	e Br−Br (a_1)	164.4[e]		v (b_1)	50.9[e]		9.37[e]	9.37
PBr_3	e (a_1)	165.9[e]		v (a_2'')	77.4[e]		9.36[e]	9.36
PF_2Cl	e F−Cl (a')	210.9	−55.0	e F−Cl (a')	152.7	−61.6	10.60	10.85
$PFCl_2$	e Cl−Cl (a_1)	205.1	−53.9	v	140.9	−21.3	10.10	10.35
PHFCl	e F−Cl (a')	204.4	−50.6	v (a'')	85.2	−16.5	9.88	10.13
PFClBr	e Cl−Br (a')	173.2[e]		e Cl−Br (a')	107.5[e]		9.99[e]	9.99

[a] Preferred inversion mode: v = vertex, e = edge. [b] QCISD(T)/6-311+G(2df,p) values, with MP2(ZPE) corrections. [c] Correlation correction to the barrier, i.e., difference of the QCISD(T) and HF energies. [d] Calculated adiabatic ionization energy at the QCISD(T)/6-311+G(2df,p) level with MP2(ZPE) corrections and predicted values for IE_a by applying a uniform correction of +0.25 eV to the QCISD(T) values and no correction to the B3LYP values; in parentheses are experimental values, eV. [e] B3LYP/6-311+G(2df,p) values, with B3LYP(ZPE) corrections.

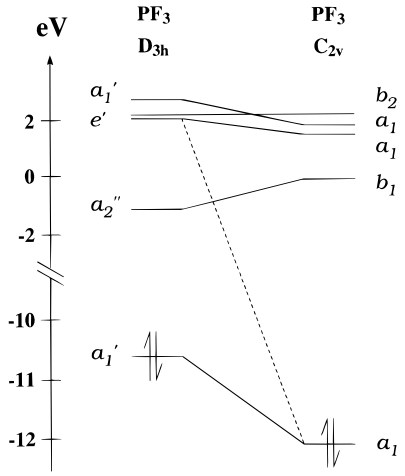

Figure 3. Orbital correlation diagram upon distortion of D_{3h} PF_3 to C_{2v} PF_3.

ΔEN(P−X) values for the compounds under consideration. While only PH_3 has an a_2'' HOMO, the perhalogenated phosphines PBr_3, PCl_3, and PF_3 have an a_1' HOMO. As the difference in electronegativity changes throughout the series, the a_1' orbital gets stabilized, while the a_2'' orbital destabilized. Note that the molecules that have in their D_{3h} form an a_1' HOMO systematically undergo inversion through a T-shaped edge form (see Table 6). This also holds for their ionized counterparts.

3.4. The Pseudo-Jahn−Teller Effect. Table 6 summarizes the preferred inversion pathways of the substituted phosphines examined. This table will be taken as a guideline for the discussion through this section.

As noted in the Introduction, the edge inversion TS can be understood by a pseudo-Jahn−Teller distortion of the vertex form. Let us consider the trigonal planar D_{3h} structures. Due to an $a_1' \otimes e'$ mixing, the D_{3h} form can distort into a T-shaped C_{2v} structure. This clearly happens for PF_3, $PF_3^{\bullet+}$, PCl_3, and PBr_3. This effect is exemplified for D_{3h} PF_3 in Figure 3. This orbital correlation diagram correlates the orbitals of the D_{3h} form with those of the C_{2v} form. It is thus seen that the a_1' HOMO (D_{3h}) receives considerable stabilization by interaction with the unoccupied e' orbital. In both $PCl_3^{\bullet+}$ and $PBr_3^{\bullet+}$, which have an a_2'' SOMO in their D_{3h} form, such a distortion does not seem possible. As a consequence, the latter two species undergo inversion via the classical umbrella mode.

When considering the species with gradual or mixed substitution, much the same thing happens. However, the concept of symmetry lowering cannot be fully applied because the highest possible symmetry is only C_{2v}. For instance, it is not possible to locate a near D_{3h} form with an a_1 or a' HOMO (depending on whether the symmetry is C_{2v} or C_s), since such a starting point for a geometry optimization immediately leads to the corresponding edge form. As such, strictly speaking, it is not appropriate to evoke a pseudo-Jahn−Teller effect. It is however convenient to consider the mono-, di-, and mixed substituted species as lower symmetry analogues of PX_3 compounds, and hence, a similar phenomenon does occur.

Finally, it is important to note some trends in the inversion behavior of the phosphines under consideration. Monosubstituted, neutral phosphines consistently undergo inversion via the classical way, even though the nonclassical alternative already exists, while the corresponding species with two halogen (X) atoms proceed through the edge X−X form. The ionized species, as shown by Table 6, clearly have a general propensity for vertex inversion pathways. Only in a few cases with strong presence of halogen atoms ($PF_3^{\bullet+}$, $PF_2Cl^{\bullet+}$, $PFCl_2^{\bullet+}$, and $PFClBr^{\bullet+}$) does inversion occur through an edge TS, but the energy differences between both vertex and edge TS are substantially reduced. The fact that the HOMO is only singly occupied in these radical cations markedly diminishes the strength of the pseudo-Jahn−Teller effect. One can thus conclude that the strength of the pseudo-JT effect increases with increasing degree of halogen substitution and with increasing electronegativity of the particular halogen atom. The latter conclusion may tentatively be deduced from the fact that $PF_3^{\bullet+}$ undergoes edge inversion, while $PCl_3^{\bullet+}$ and $PBr_3^{\bullet+}$ invert via the umbrella mode. A third factor concerns the occupation number of the HOMO. Neutral species, where the HOMO is doubly occupied, more easily choose the edge path, whereas the cations tend to vertex paths.

3.5. Correlation Effect on Calculated Inversion Barriers. As with the computation of other molecular properties, the question of the contribution of electron correlation to barriers

has been posed from the early stage. On the basis of the Brillouin and Hellmann−Feynman theorems, Freed[37] suggested in 1968 that the barriers can be considered in the class of one-electron operators and thus obtained correctly through first-order Hartree−Fock wave functions. The resulting errors are therefore of second-order. In an earlier survey of computed barriers for first-row hybrids,[5] it was stated that "the correlation energy changes associated with inversion barriers...are usually several tenths kcal/mol and may be as great as 1 kcal/mol. Whether or not this effect is important depends on the size of the SCF barriers."[5] Subsequent studies[8,9,29] concur with this observation. For second-row hydrides, the correlation corrections are somewhat larger (up to 12 kJ/mol), but the trend is different. Thus, electron correlation tends to increase the barriers in the first-row hydrides but decreases them in second-row hydrides. For larger pyramidal species, comprehensive studies on the correlation effect are rather scarce.[38]

Table 6 records the calculated inversion barriers of the various phosphines along with the correlation corrections. On one hand, these results confirm the trend noted above for PH_3 and $PH_3^{\bullet+}$. The correlation corrections are rather small and negative. On the other hand, substantial corrections for substituted phosphines are revealed, in particular in halogenated derivatives. In PF_3 and PCl_3, the reduction of the barrier upon incorporation of electron correlation amounts to no less than 64 kJ/mol. Due to the strong mixing of frontier orbitals, it is clear that the barriers in these pyramidal species can no longer be treated as first-order operators, and as a consequence, Freed's suggestion is no longer valid.

4. Conclusions

In summary, the inversion process in phosphines (R_3P) and their radical cations has been studied using both high-level ab initio MO and DFT techniques. It appears, as noted previously, that two distinct inversion pathways exist. While the vertex inversion corresponds to the classical well-known umbrella mode, the edge inversion is characterized by a T-shaped transition structure and can be understood as a pseudo-Jahn−Teller distorted form of the corresponding vertex form. The following trends were noted.

(i) None of the PH_3, $PH_3^{\bullet+}$, or methyl-substituted species $PH_x(CH_3)_y$ and their radical cations undergo edge inversion. They all prefer a vertex path, which lies considerably lower than the edge path (380−480 kJ/mol for the neutral species, 300−350 kJ/mol for the cations). Hence we feel safe to conclude that methyl substitution, and probably alkyl substitution in general, has no effect on the inversion behavior of both PH_3 and $PH_3^{\bullet+}$.

(ii) Concerning the monosubstituted halogenated species (PH_2X and $PH_2X^{\bullet+}$), it is seen that, although vertex inversion is still largely preferred, the edge inversion begins to take place in both neutral and ionized states.

(iii) Disubstituted neutral halogenated species (PHX_2) are the first in the series to follow edge inversion rather than the classical umbrella mode. Their corresponding racical cations $PHX_2^{\bullet+}$, however, invert through vertex forms. One mixed disubstituted form has also been studied, PHFCl, where the same behavior is seen: the neutral form chooses edge inversion, while the cation proceeds through the vertex TS. Note, however, that the most favorable edge TS of PHFCl is the one with the H atom in equatorial position.

(iv) All trihalogenated neutral species undergo edge inversion, while among their radical cations, only $PF_3^{\bullet+}$, $PF_2Cl^{\bullet+}$, and $PFClBr^{\bullet+}$ do so. It is shown for PX_3 species that the D_{3h} form with a_1' HOMO symmetry is unstable with respect to a pseudo-Jahn−Teller distortion ($a_1'\otimes e'$ mixing) to the more stable T-shaped C_{2v} edge form. This can be generalized to other species with edge inversion, in the sense that they behave as lower symmetry analogues of the PX_3 ones. Our results show that the pseudo-JT effect grows stronger with (i) increasing number of halogen atoms, (ii) increasing electronegativity of the halogen atoms, and (iii) with increasing occupation number of the HOMO. The latter effect is also the reason that the energy difference between edge and vertex forms is considerably smaller in the cations than in the corresponding neutral species.

(v) Irrespective of the inversion mode, the barrier heights are markedly reduced following ionization.

Finally, one might wonder about the inversional behavior of phosphines containing group V or VI elements, such as $PH_x(OR)_y$ or $PH_x(NR_2)_y$, with $x + y = 3$. Based on electronegativity arguments, N-containing substituents are expected to behave similarly to Cl, and O to that in between F and Cl. In fact, we have been able to obtain a stable edge form for the $P(OH)_3$ molecule, albeit at a low level of theory. Note, however, that it is rather dangerous to speculate on the inversional behavior of these compounds, due to the following reasons.

(a) Since group V and VI substituents themselves bear substituents, the electronic effect of the latter should also be taken into account.

(b) In the case of OH groups or NH_2 groups, it is likely that the edge inversion structures may gain an additional stabilization by internal hydrogen bonding.

(c) The R substituents give rise to steric congestion in the transition structures, especially the edge-like ones, making the analysis more complicated.

A few more other conclusions resulted as "byproducts" of this study. By investigating the effect of electron correlation on the energy barriers, it was shown that, for di- and trihalogenated phosphines, Freed's suggestion is no longer valid. Another point of interest concerns the relative performance of DFT with respect to the ab initio MO methods. For the barrier heights, it is seen that B3LYP is often in better accordance with QCISD(T)/6-311+G(2df,p) than is MP2. Furthermore, the differences between B3LYP results with small and large basis sets is rather small, as expected. However, some remarkable qualitative discrepancies with MP2 occur as to the number of imaginary vibrations of certain nonequilibrium structures. It is often seen, in particular for structures with two or three imaginary wavenumbers, that MP2 tends to yield a smaller number of imaginary wavenumbers. In most of these cases, it is the vibration corresponding to the inversion mode that loses its imaginary character at the MP2 level. As noted in the text, it is not clear to us whether we should attribute this to a MP2 or B3LYP deficiency. The overall qualitative conclusions drawn from B3LYP or QCISD(T) calculations, i.e., as to which inversion mode is the preferred one, coincide in all but one case ($PFCl_2^{\bullet+}$). Hence, B3LYP-DFT again proves to be a valuable method for treating phosphorus-containing systems.[39] The calculated ionization energies are also tabulated in Table 6. As expected, the computed QCISD(T) values for PH_3 and PF_3 are about 0.2−0.3 eV too small with respect to the PES values. The B3LYP value for PH_3, however, is 9.82 eV, and for PF_3 it is 11.47 eV. Assuming a certain systematic error of the calculated values, more realistic ionization energies of other phosphines can thus be derived by adding a uniform correction of +0.25 eV to the QCISD(T) values. Since little is known about the performance of B3LYP for ionization energies, no

correction was applied to them. These predicted values are also listed in Table 6.

Acknowledgment. The authors thank the FWO-Vlaanderen and the KULeuven Research Council (GOA program) for continuing support.

Supporting Information Available: Optimized structures of all species considered at the B3LYP and MP2 level (17 pages). Ordering information is given on any current masthead page.

References and Notes

(1) Clementi, E. *J. Chem. Phys.* **1967**, *46*, 3851.
(2) Rauk, A.; Allen, L. C.; Clementi, E. *J. Chem. Phys.* **1970**, *52*, 4133 and references therein.
(3) Lehn, J. M. *Top. Curr. Chem.* **1970**, *15*, 311.
(4) Golebiewski, A.; Parczewski, A. *Chem. Rev.* **1974**, *74*, 519.
(5) Veillard, A. In *Quantum Mechanics of Molecular Conformations*; Pullmann, B., Ed.; John Wiley: New York, 1975.
(6) Papousek, D.; Spirko, V. *Top. Curr. Chem.* **1976**, *68*, 59.
(7) Payne, P. W.; Allen, L. C. in *Modern Theoretical Chemistry*, Schaefer, H. F., Ed.; Plenum Press: New York, 1977; Vol. 4.
(8) Rush, D. J.; Wiberg, K. B. *J. Phys. Chem. A* **1997**, *101*, 3143.
(9) Lee, J. S. *J. Phys. Chem. A* **1997**, *101*, 8762.
(10) Schmidekamp, A.; Skaarup, S.; Pulay, P.; Boggs, J. E. *J. Chem. Phys.* **1977**, *66*, 5769.
(11) Boggs, J. E.; Seida, D. *J. Chem. Phys.* **1981**, *75*, 3645.
(12) Marynick, D. S. *J. Chem. Phys.* **1980**, *73*, 3939.
(13) Dixon, D. A.; Arduengo, A. J., III; Fukunaga, T. *J. Am. Chem. Soc.* **1986**, *108*, 2461.
(14) Dixon, D. A.; Arduengo, A. J., III. *J. Am. Chem. Soc.* **1987**, *109*, 338.
(15) Dixon, D. A.; Arduengo, A. J., III. *J. Chem. Soc., Chem. Commun.* 1987; p 498.
(16) Gutsev, G. L. *J. Chem. Phys.* **1993**, *98*, 444.
(17) Schwerdtfeger, P.; Boyd, P. D. W.; Fischer, T.; Hunt, P.; Lidell, M. *J. Am. Chem. Soc.* **1994**, *116*, 9620.
(18) Clotet, A.; Rubio, J.; Illas, F. *J. Mol. Struct. (THEOCHEM)* **1988**, *164*, 351.
(19) Minyaev, R. M. *J. Mol. Struct. (THEOCHEM)* **1992**, *262*, 79.
(20) Minyaev, R. M.; Wales, D. J.; Walsh, T. R. *J. Phys. Chem.* **1997**, *101*, 1384.
(21) Creve, S.; Nguyen, M. T. *Chem. Phys. Lett.* **1997**, *273*, 199.
(22) Moc, J.; Morokuma, K. *Inorg. Chem.* **1994**, *33*, 551.
(23) Marynick, D. S.; Rosen, D. C.; Liebman, J. F. *J. Mol. Struct. (THEOCHEM)* **1983**, *94*, 47.
(24) Edgecombe, K. E. *J. Mol. Struct. (THEOCHEM)* **1991**, *226*, 157.
(25) Frisch, M. J.; Trucks, G. W.; Schlegel, H. B.; Gill, P. M. W.; Johnson, B. G.; Wong, M. W.; Foresman, J. B.; Robb, M. A.; Head-Gordon, M.; Replogle, E. S.; Gomperts, R.; Andres, J. L.; Raghavachari, K.; Binkley, J. S.; Gonzalez, C.; Martin, R. L.; Fox, D. J.; Defrees, D. J.; Baker, J.; Stewart, J. J. P.; Pople, J. A. *GAUSSIAN 94, Rev. C.3*; Gaussian: Pittsburgh, 1995.
(26) Scott, A. P.; Radom, L. *J. Phys. Chem.* **1996**, *100*, 16502.
(27) Weston, R. E. *J. Am. Chem. Soc.* **1954**, *76*, 2645.
(28) Spirko, V.; Civis, S.; Ebert, M.; Danielis, V. *J. Mol. Spectrosc.* **1986**, *119*, 425.
(29) Marynick, D. S.; Dixon, D. A. *J. Phys. Chem.* **1982**, *86*, 914.
(30) Maier, J. P.; Turner, D. W. *J. Chem. Soc., Faraday Trans. 2* **1972**, *68*, 711.
(31) Maripiu, R.; Reineck, I.; Agren, H.; Wu, N. Z.; Wi, M. R.; Veenhuizen, H.; Al-Shamma, S. H.; Karlsson, L.; Siegbahn, K. *Mol. Phys.* **1983**, *48*, 1255.
(32) Marynick, D. S. *J. Chem. Phys.* **1981**, *74*, 5186.
(33) Aarons, J.; Guest, M. F.; Hall, M. B.; Hiller, I. H. *J. Chem. Soc., Faraday Trans. 2* **1973**, *69*, 643.
(34) Kölmel, C.; Ochsenfeld, C.; Ahlrichs, R. *Theor. Chim. Acta* **1991**, *82*, 271.
(35) Fades, R. A.; Well, D. A.; Dixon, D. A.; Douglass, C. A. *J. Phys. Chem.* **1981**, *85*, 976.
(36) Halpern, A. M.; Ondrechon, M. J.; Ziegler, L. D. *J. Am. Chem. Soc.* **1986**, *108*, 3907.
(37) Freed, K. F. *Chem. Phys. Lett.* **1968**, *2*, 255.
(38) Nguyen, M. T.; Ha, T. K. *Chem. Phys. Lett.* **1986**, *123*, 537.
(39) Nguyen, M. T.; Creve, S.; Vanquickenborne, L. G. *J. Chem. Phys.* **1996**, *105*, 1922.